Solid Freeform Fabrication 2022: Proceedings of the 33rd Annual International Solid Freeform Fabrication Symposium – An Additive Manufacturing Conference

STUDY OF DIFFERENT AGING CONDITIONS FOR ANALYSIS OF MICROSTRUCTURE AND MECHANICAL PROPERTIES OF F357 ALLOY FABRICATED IN LPBF PRINTER

V.A. Medrano[1,2], K. Caballero[1,2], E. Arrieta[1,2], M. Benedict[3], R.B. Wicker[1,2], and F. Medina[1,2]

[1] W.M. Keck Center for 3D Innovation, The University of Texas at El Paso, El Paso, TX 79968, USA
[2] Department of Aerospace and Mechanical Engineering, The University of Texas at El Paso, TX 79968, USA
[3] Air Force Research Laboratory, Wright-Patterson Air Force Base, Dayton, OH, 45433, USA

Keywords: additive manufacturing, LPBF, F357, aging, aluminum.

ABSTRACT

Aluminum F357 is a widely used material for casting in aerospace and additive manufacturing industry. Heat treatments are commonly applied to some aluminum alloys to modify its properties. With a further study on the aging and performance of the F357 with 3D printing technology, several industries benefit of this, military, automotive and aerospace are some examples, because the numerous components casted in service. This work presents mechanical properties of F357 specimens fabricated with EOS technology and subjected to heat treatments. Heat treatments conditions were applied to tensile specimens and tested. Furthermore, the specimens were subjected to artificial thermal aging for 100 h and 1000 h at two different temperatures (285 ºF and 350 ºF), and their mechanical properties were also determined. Finally, remarks on the comparison between the heat treatments and the effect of thermal aging on the microstructures and mechanical properties of the specimens will be presented.

1 INTRODUCTION

The study of aluminum microstructure and mechanical properties is of interest since this metal is among one of the most abundant elements on Earth and its properties turn aluminum into a convenient material for variety of applications. According to Rashad, et al. [1], Tsaknopoulos, et al. [2] and Dahle, et al. [3] various heat treatments and many other metals such as silicon, magnesium, titanium, and chrome are applied to aluminum to change its mechanical properties and microstructure, making it better for different cases and applications. Among aluminum-silicon castings, there is aluminum F357 (AlSi7Mg), a lightweight alloy (2.67 g/cm^3 density), the F357 has been a big part of engineering and manufacturing over the past decades, turning it into one of the most used metals for aircraft parts and aerospace components. In addition, many other aluminum alloys are constantly used in many other industrial processes, some of the applications of aluminum include the fabrication of automotive components such as heat exchangers, chassis frames, and bodywork. These components usually keep a geometry which is reachable with classic manufacturing processes such as pressure die casting, nevertheless, some other components require more complex geometries and classic manufacturing methods usually present limitations to these complex geometries since they often produce undesired defects such as porosity on critical areas. With the relatively new appearance of metal additive manufacturing, specifically Laser Powder Bed Fusion (LPBF) technology, these limitations have been largely overcome since many parameters (layer thickness, hatch distance, energy density, etc.) can be modified in order to reduce the appearance of undesired defects. LPBF fabricated parts of aluminum F357 have shown a nominal yield stress (YS) of 400 MPa, in contrast with 170 MPa for cast parts [4] [5].

2 MATERIALS AND METHODS

2.1 Methods

There is currently no ASTM standard for treating aluminum F357, however, ASTM F3318 standard will be followed for heat treating F357. Studies have shown the modification of microstructure and of the mechanical properties at room temperature (25 °C) of laser powder bed fusion aluminum F357 parts involve variety of post-process heat treatments. In this work, following heat treatments will be applied to the F357: NHT condition (no heat treatment required), stress relief (SR) anneals at 285 °C held for 120 min (±15 min) and cooled at a rate equal to air cooling or faster, T6 condition held at 530 °C for 360 min, then quenched in water or glycol and aged at 160 °C for 360 min and hot isostatic pressing condition (HIP) under an inert atmosphere at 100 MPa, ~515 °C and HIP + T6 condition. In addition, since it is of interest knowing the performance of the F357 under service conditions, artificial thermal aging will be held on some of the specimens to observe the changes in microstructure and mechanical properties. The aging will be divided into two different temperatures, 285 °F (~140 °C) and 350 °F (~177 °C) and three different aging times will be held (0 h, 100 h and 1000 h). The resulting microstructures will be characterized by optical metallography and associated mechanical properties, including room temperature tensile tests and Vickers micro-indentation hardness measurements. Knowing that 5 heat treatments and 5 different aging conditions will be applied to the specimens, this work will present results for up to 100 different variants from the F357.

2.2 Powder feedstocks

The powder utilized in this research was atomized F357 (AlSi7Mg) shown in Figure 1 and Figure 2 provided by Valimet, AM 357C. A Retsch Camsizer X2 (Haan, Germany) was used in order to study particle size and shape of the powder through dynamic image analysis with a two-camera-system, the Camsizer yields **consistent** particle size distribution and shape analysis. The stock powder had a particle size distribution of D10: 24.4 μm, D50: 39.3 μm, and D90: 60.4 μm. **How is it consistent? Vs what or how?**

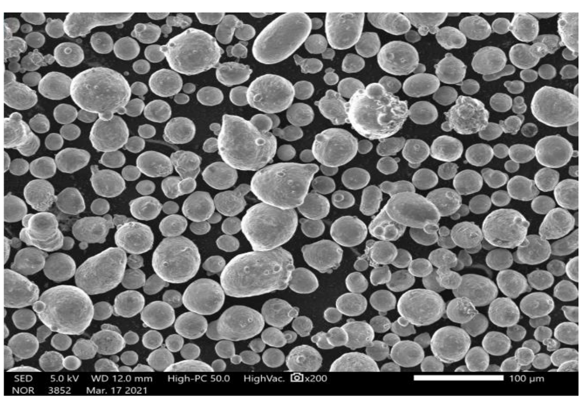

Figure 1

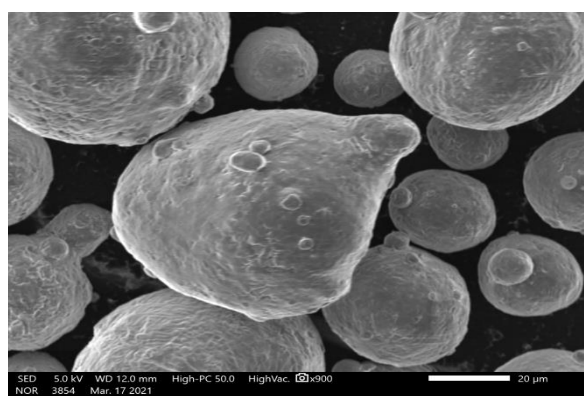

Figure 2

2.3 Laser powder fusion system and process parameters.
The printed specimens were fabricated using an EOS M290 (Kralling, Germany). The M920 is equipped with a 400 W Ytterbium fiber laser and a 250 x 250 x 325 build volume. The F357 alloy was fabricated using a laser power of 370 W, a scan speed of 1300 mm/s, hatch of 0.13 mm, stripe of 7 mm, layer thickness of 30 μm and energy density of 73 J/mm^3. In addition, printed parts were provided to us in order to heat treat, age and test, these previously mentioned parts were printed using an SLM 125 HL printer which has a build size of 125 x 125 x 75 mm. The parameters used on these parts were the following: scan speed of 1225 mm/s, laser power of 370 W, hatch of 0.17 mm, layer thickness of 30 μm and energy density of 59.2 J/mm^3.

2.4 Tensile testing
Tensile testing is performed on all samples using an MTS Landmark (Eden Praire, US) servo-hydraulic system which has a force capacity of 100 kN. The system is equipped with threaded grips where the specimens are placed. In addition, an MTS 30mm axial clip extensometer is used. All samples are machined following ASTM E8 standard. Speed of testing was controlled by crosshead displacement speed of 0.476 mm/min.

Figure 3

Figure 4

2.5 Density measurements
Density measurements are obtained through helium gas displacement method with an Accupyc II 1340 Pycnometer (Norcross, United States). The pycnometer performs 10 measurements for each experimental variant. Mass measurements are obtained using a Sartorius CP124S weight balance (Sartorius AG, Germany). Density is then calculated with the resulting mass and volume measurements.

2.6 Microstructure characterization
After the tensile test has been performed, the fracture is protected and then the thread part of the specimen is sectioned into three different planes: Y-Z, X-Z, and X-Y planes. Once sectioned, an ATM OPAL 460 (Haan, Germany) hot mounting press is used to create metallographic samples out of phenolic powder and back epoxy. Once mounted, the samples are ground and polished as shown in Figure 3 with an ATM SAPHIR 530 semi-automatic system.

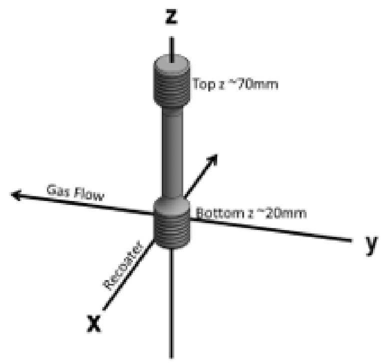

Figure 5

The sample preparation starts with the ground of samples with silicon carbide grinding papers of 320 grit at 300 rpm with 25 N of force and after 1 min of grinding the paper is changed to 800 grit paper, using the same presets, and using continuous water while the machine is running. The samples are then moved to an abrasive diamond disc and ground with a 9 µm diamond suspension at 150 rpm with 25 N of force for 3:30 min. Once this step is finished, the samples will be polished using a woven white wool cloth with a 3 µm diamond suspension at 150 rpm with 20 N of force for 5 min. Samples were finally polished using 0.2 µm fumed silica at 150 rpm with 15 N of force for 10 min.

The microstructure is revealed using Keller's etchant as shown in Figure 4, this etchant consisted of 5 mL of Nitric Acid, 3 mL of Hydrochloric Acid, 2 mL of Hydrofluoric Acid, and 190 mL of Distilled Water. The submersion method was used for a range of 36 s to 39 s. All optical micrographs were taken on an Olympus GX53 (Olympus Inc., Tokyo, Japan) inverted optical microscope.

Figure 6

Figure 7

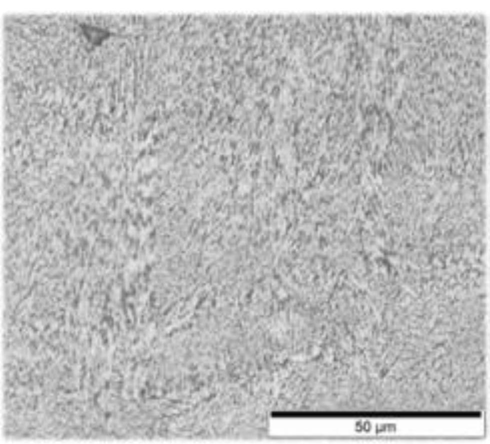

Figure 8

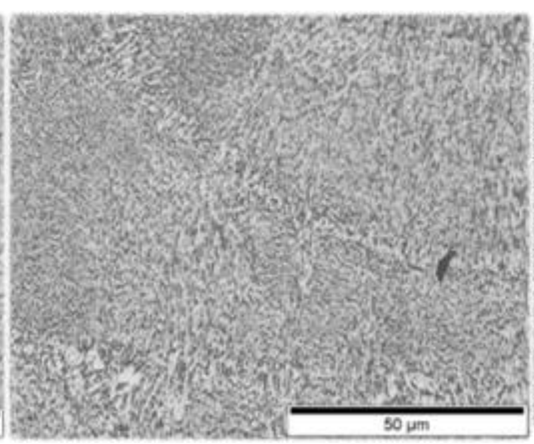

Figure 9

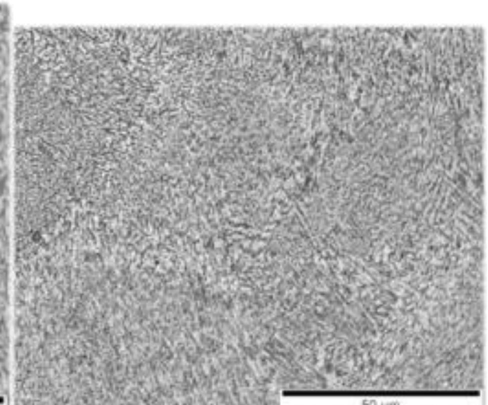

Figure 10

3 RESULTS AND DISCUSSION

3.1 Stress relief results

It was shown that yield strengths increased by approximately 15% after 1000 hours of aging at 350 °F. This observation was consistent regardless of the printing orientation and manufacturer. In addition, there was no remarkable change on the yield strengths after 1000 hours of aging at 285 °F and once again, this kept true regardless of orientation and manufacturer. Shown in Table 1 are the results of yield stress, ultimate tensile strength, and maximum strain. Comparing both XY and Z-orientation specimens, we can see that yield stress at 100 hours of aging at any temperature goes from 22.6 kip to 23.7 kip. If we observe specimens subjected to 1000 hours of aging at 285 °F, we will see a decrease in the yield stress (22.6 kip to 21.5 kip). On the other hand, if we observe specimens subjected to 1000 hours of aging at 350 °F, an increase in the yield stress can be denoted (22.6 kip to 26.1 kip). In addition, if we observe 0 hours of aging specimens, we will see UTS values ranging from 34.9 kip to 36.6 kip, while specimens subjected to 1000 hours of aging at 350 °F show an increase in the UTS with values up to 36.9 kip. Respecting to the maximum strain there was an increase in the elongation after 100 hours of aging at any temperature, 0 hours of aging show values ranging 16.3% elongation while specimens subjected to 100 or more hours of aging at any temperature show elongations of up to 21.6%. Table 2 – 5 represent in a better way the change in the mechanical properties of the F357 after stress relief and aging.

					σ_Y (ksi)	STDEV.P σ_Y (ksi)	UTS (Ksi)	STDEV.P UTS (Ksi)	ε_{max} (%)	STDEV.P ε_{max} (%)
SR1	Z-Orientation	285	0hr	EOS	23.0	0.51	36.2	1.47	18.2	1.54
		285	100hr	EOS	25.7	0.54	39.5	0.75	17.5	3.61
		285	1000hr	EOS	23.2	0.49	35.7	0.88	18.1	2.21
		350	*0hr*	*EOS*	*23.0*	*0.51*	*36.2*	*1.47*	*18.2*	*1.54*
		350	*100hr*	*EOS*	*25.5*	*0.97*	*37.5*	*1.34*	*23.1*	*1.41*
		350	*1000hr*	*EOS*	*27.5*	*0.60*	*40.4*	*0.88*	*23.1*	*1.01*
	XY-Orientation	285	0hr	EOS	23.6	0.26	36.1	0.19	20.4	1.01
		285	100hr	EOS	24.6	0.92	36.5	1.07	23.8	1.40
		285	1000hr	EOS	23.5	0.33	33.1	4.36	24.5	0.68
		350	*0hr*	*EOS*	*23.6*	*0.26*	*36.1*	*0.19*	*20.4*	*1.01*
		350	*100hr*	*EOS*	*25.5*	*0.97*	*37.5*	*1.34*	*23.1*	*1.41*
		350	*1000hr*	*EOS*	*27.5*	*0.60*	*40.4*	*0.88*	*23.1*	*1.01*

Table 1. Mechanical Results for EOS printed parts with SR1 HT.

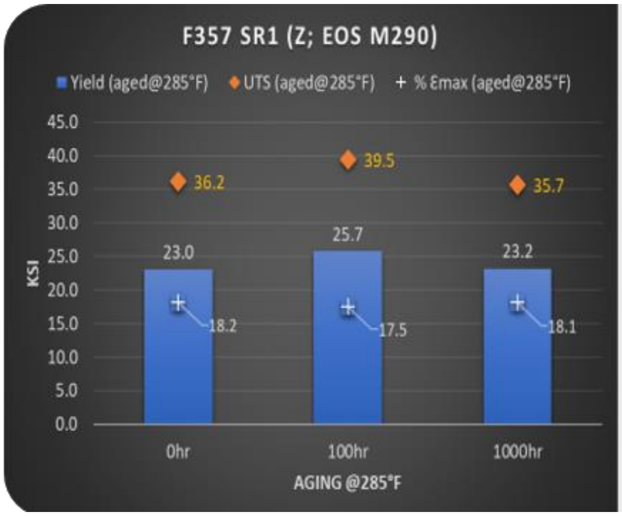

Table 2. Mechanical Results SR1 HT at 285F in Z orientation

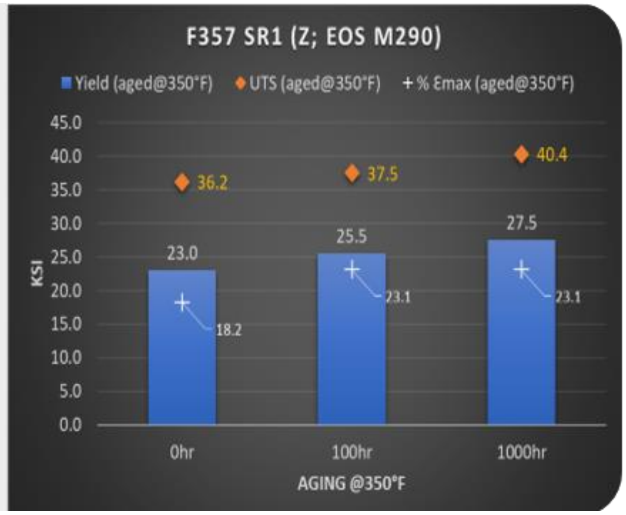

Table 3. Mechanical Results SR1 HT at 350F in Z orientation

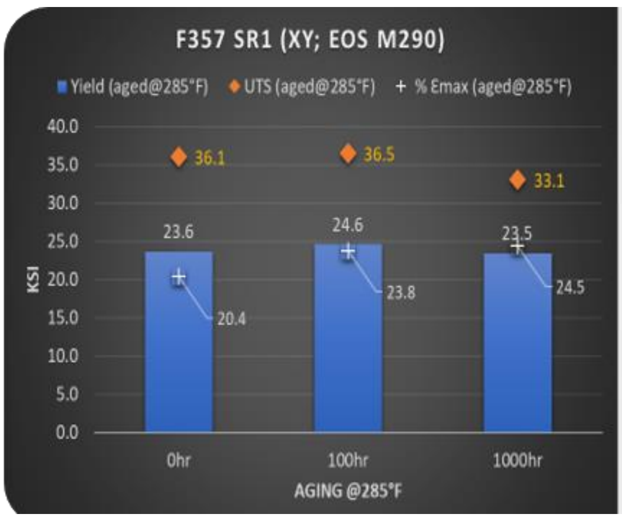

Table 4. Mechanical Results SR1 HT at 285F in XY orientation

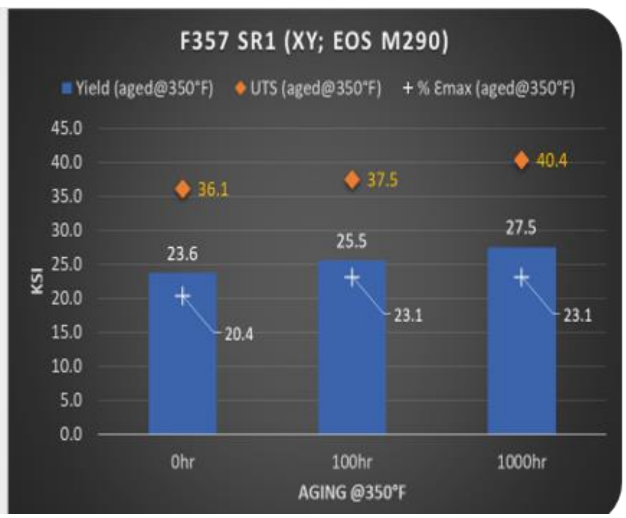

Table 5. Mechanical Results SR1 HT at 350F in XY orientation

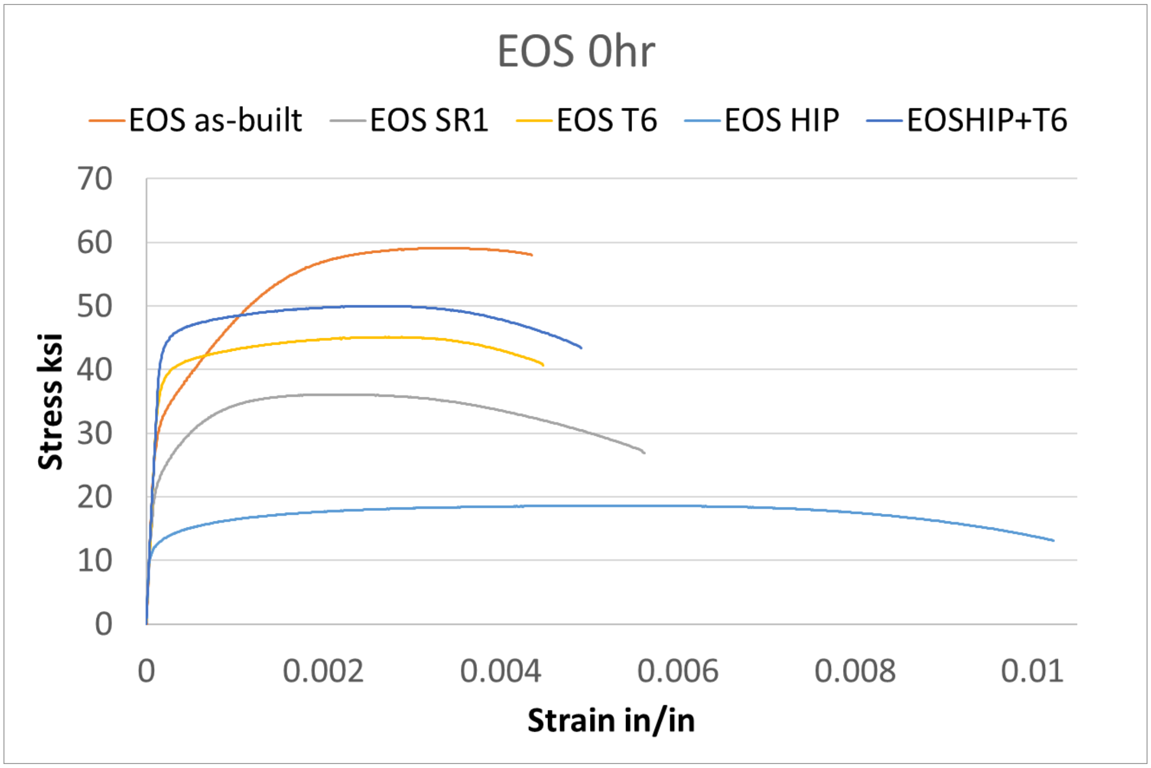

Graph 1. Characteristic curves for EOS printed parts in Z orientation at 0hrs.

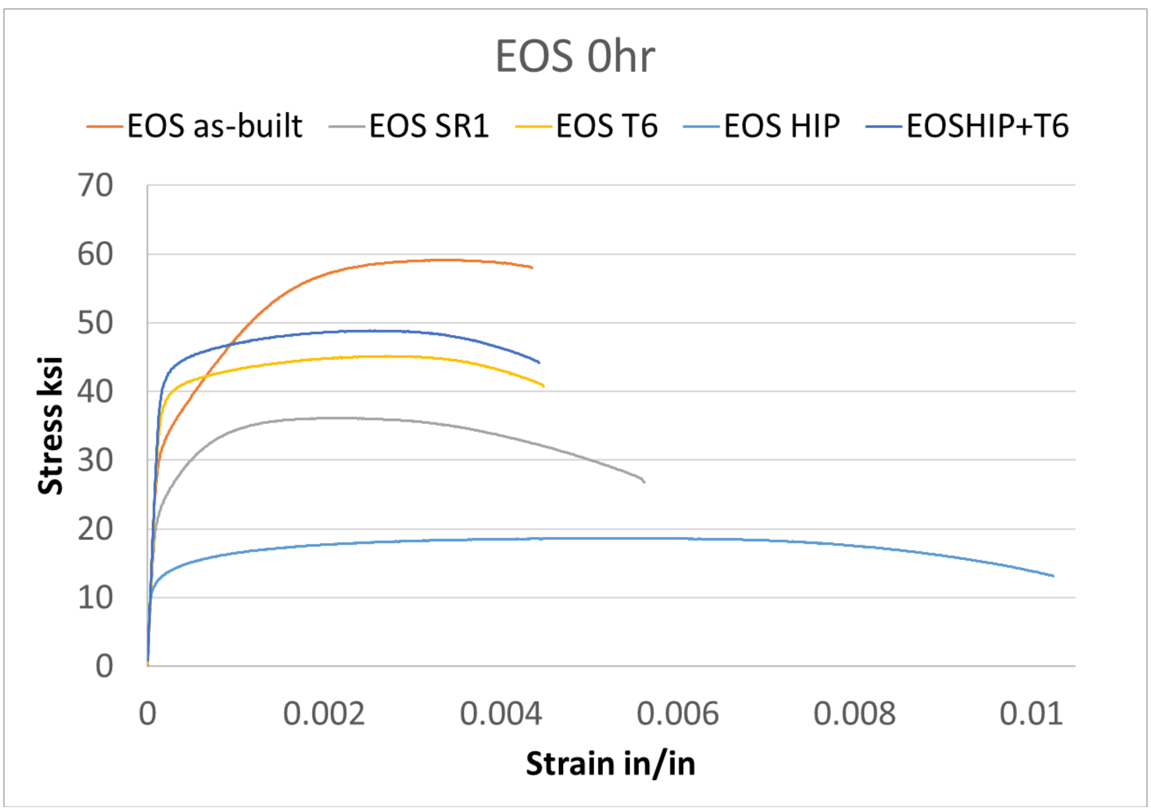

Graph 2. Characteristic curves for EOS printed parts in XY orientation at 0hrs.

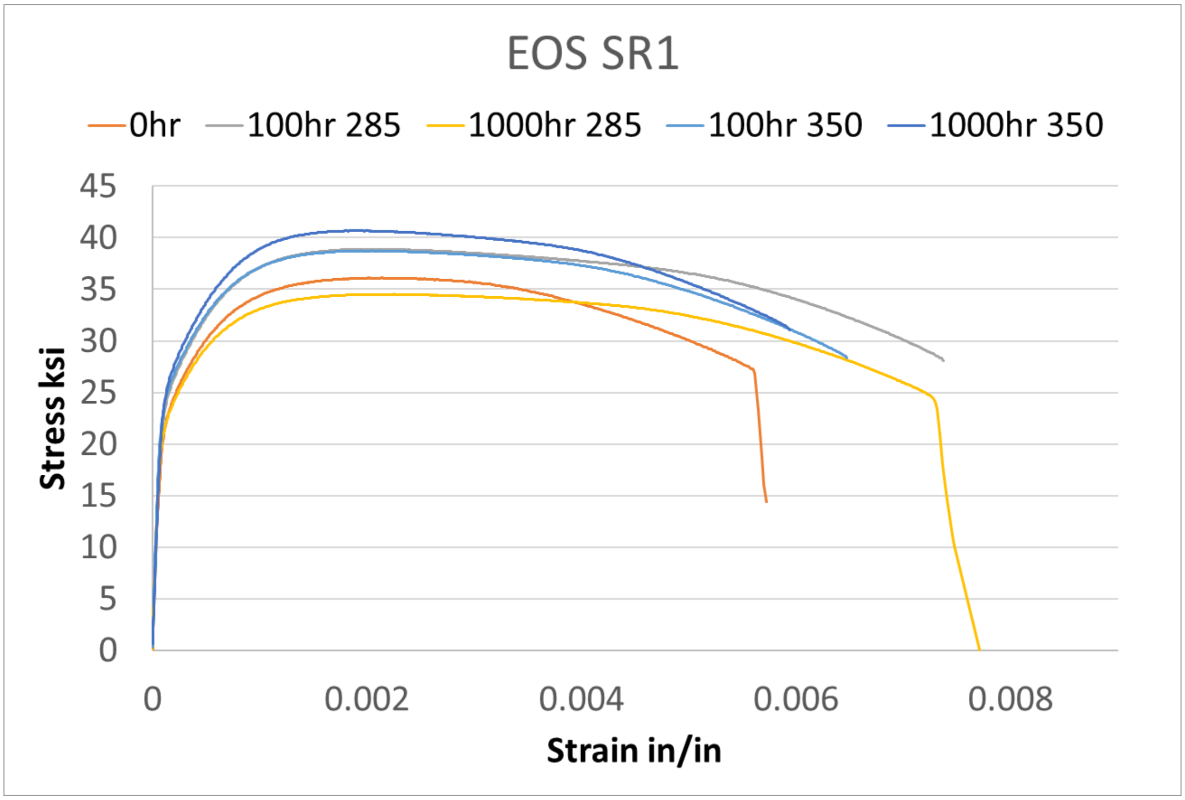

Graph 3. Characteristic curves for EOS printed parts in Z orientation with SR1 HT.

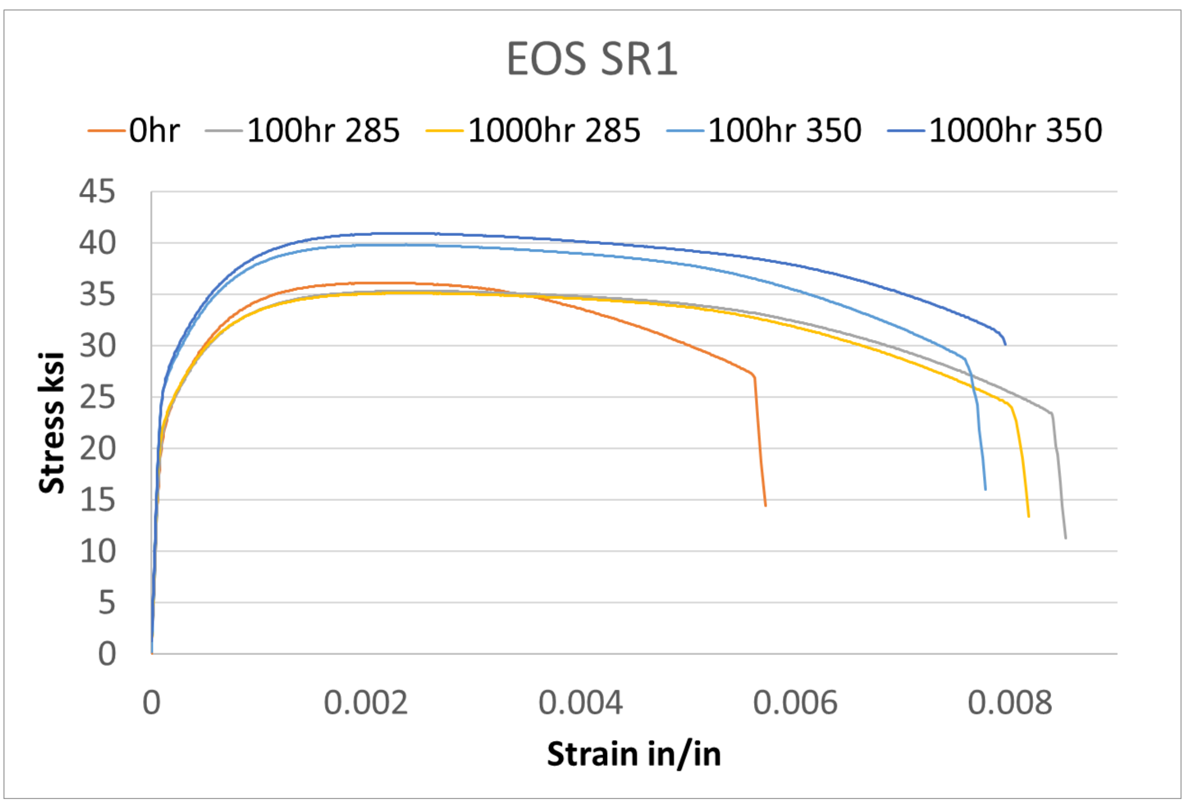

Graph 4. Characteristic curves for EOS printed parts in XY orientation with SR1 HT.

It is shown that there is no significant difference between the EOS printed samples at 0hr with XY orientation and the same samples at Z orientation, base on Graph 1 and Graph 2, the characteristic curves are basically the same regardless the orientation these were printed.
In other hand, we can compare these two graphs with Graph 3 and Graph 4, where we can see the characteristic curves for printed parts in XY and Z orientation, with the different aging conditions in both graphs.

3.1.1 Density results

Results showed that density was persistent along every SR1 variation. The density for aluminum F357 is 2.67 g/cm^3 and our helium pycnometry results threw values varying from 2.533 to 2.6585 g/cm^3. Shown in Table 6 and Table 7 are the results of the helium pycnometry.

	0 h	0 h	100 h	100 h	1000 h	1000 h
	XY	Z	XY	Z	XY	Z
SR1	2.6525	2.6500	2.6553	2.6450	2.6566	2.6561
	2.6486	2.6519	2.6475	2.6552	2.6519	2.6541

Table 6. SR1 aging at 285 °F (~140 °C) (values on top are for EOS, bottom values are for SLM)

	0 h	0 h	100 h	100 h	1000 h	1000 h
	XY	Z	XY	Z	XY	Z
SR1	N/A	N/A	2.6545	2.6565	2.533	2.6541
	N/A	N/A	2.6545	2.6550	2.6478	2.6585

Table 7. SR1 aging at 350 °F (~177 °C) (values on top are for EOS, bottom values are for SLM)

3.2 Summary and conclusions

The work here presented observed the effects of heat treatments and aging conditions to the mechanical properties and microstructure of LPBF fabricated F357 alloy. NHT condition, stress relief, hot isostatic pressing, T6 and HIP+T6 conditions were applied to our specimens. In addition, our specimens were also subjected different aging conditions: 285 °F (~140 °C) and 350 °F (~177 °C) and three different aging times (0 h, 100 h and 1000 h).

Tensile test results for stress relief variations showed that after 1000 hours of aging at 350 °F, yield strengths increased by 15%, this kept true regardless of printing orientation and manufacturer. Finally, there was no remarkable change on the yield strengths of the specimens after 1000 hours of aging at 285 °F. Ultimate tensile strength and maximum strain also experienced changes, it was observed that UTS increased by 3% after 1000 hours of aging at 350 °F and maximum strain percentages reached values up to 21.6% after 1000 hours of aging at 285 °F. Respecting to the helium displacement pycnometry tests, density values ranged from 2.533 to 2.6585 g/cm^3 in comparison to the theoretical density of F357 (2.67 g/cm^3).

For the Graph 3 and Graph 4, the difference in the aging temperature has a significant effect, is a small increase in elongation for the 100hr and 1000hr at the aging temperature of 285 °F, meaning the aging make it more ductile, where we can see an increase in time of 2 minutes on the 100hr of both aging temperatures, 285 °F and 350 °F, then for the 1000hr at 285°F it only increase 1 minute for the breaking point, and for the 1000hr at 350°F increase 3 minutes and 15 seconds, being the maximum increment in time for this specific heat treatment.

Based on our results, we concluded that 1000 hours of aging at 350 °F results useful for increasing yield stress as well as ultimate tensile strength, on the other hand, 1000 hours of aging at 285 °F results useful for increasing maximum strain percentages. These observations were consistent regardless of the printing orientation and manufacturer.

References

[1] Rashad, Muhammad, Fusheng Pan, Aitao Tang, Muhammad Asif, Shahid Hussain, Jun Gou, and Jianjun Mao. 2015. "Improved Strength and Ductility of Magnesium with Addition of Aluminum and Graphene Nanoplatelets (Al+GNPs) Using Semi Powder Metallurgy Method." *Journal of Industrial and Engineering Chemistry* 23 (March): 243–50. https://doi.org/10.1016/j.jiec.2014.08.024.

[2] Tsaknopoulos, Kyle, Jack Grubbs, Matthew Siopis, Aaron Nardi, and Danielle Cote. 2021. "Microstructure and Mechanical Property Evaluation of Aluminum F357 Powder for Cold Spray Applications." *Journal of Thermal Spray Technology* 30 (3): 643–54. https://doi.org/10.1007/s11666-020-01140-4.

[3] Dahle, A. K., K. Nogita, S. D. McDonald, C. Dinnis, and L. Lu. 2005. "Eutectic Modification and Microstructure Development in Al–Si Alloys." *Materials Science and Engineering: A*, International Conference on Advances in Solidification Processes, 413–414 (December): 243–48. https://doi.org/10.1016/j.msea.2005.09.055.

[4] Möller, H., G. Govender, W. E. Stumpf, and P. C. Pistorius. 2010. "Comparison of Heat Treatment Response of Semisolid Metal Processed Alloys A356 and F357." *International Journal of Cast Metals Research* 23 (1): 37–43. https://doi.org/10.1179/174313309X451252.

[5]

ACKNOWLEDGEMENTS

The research described here was performed at The University of Texas at El Paso (UTEP) within the W.M. Keck Center for 3D Innovation (Keck Center). The authors are grateful to Jorge Merino for its guidance in the writing of this paper. Primary support for this research was provided by grant number NOAID20210005 from AFRL (Air Force Research Laboratory) as well as strategic investments via discretionary UTEP Keck Center funds and the Mr. and Mrs. MacIntosh Murchison Chair I in Engineering Endowment at UTEP. The views and opinions expressed in this article are those of the authors and do not necessarily reflect the official opinion or policy of any agency of the US government (if applicable).